MICROMAGNETIC STUDIES OF THE TRANSITION BETWEEN VORTEX AND SINGLE-DOMAIN STATES IN SUB-100 NM NANODOTS

A Senior Scholars Thesis

by

ANDREW THOMAS KING

Submitted to Honors and Undergraduate Research
Texas A&M University
in partial fulfillment of the requirements for the designation as

UNDERGRADUATE RESEARCH SCHOLAR

May 2012

Major: Physics

MICROMAGNETIC STUDIES OF THE TRANSITION BETWEEN VORTEX AND SINGLE-DOMAIN STATES IN SUB-100 NM NANODOTS

A Senior Scholars Thesis

by

ANDREW THOMAS KING

Submitted to Honors and Undergraduate Research
Texas A&M University
in partial fulfillment of the requirements for the designation as

UNDERGRADUATE RESEARCH SCHOLAR

Approved by:

Research Advisor: Igor V. Roshchin
Associate Director, Honors and Undergraduate Research: Duncan MacKenzie

May 2012

Major: Physics

ABSTRACT

Micromagnetic Studies of the Transition between Vortex and Single-Domain States in Sub-100 nm Nanodots. (May 2012)

Andrew Thomas King
Department of Physics and Astronomy
Texas A&M University

Research Advisor: Dr. Igor V. Roshchin
Department of Physics and Astronomy

Understanding energy barriers involved in nucleating and annihilating magnetic vortices in nanodots is important for magnetic memories and nano-oscillators. We used a “rigid-vortex approximation" and micromagnetic approach to calculate the total magnetic energy of a nanodot for various magnetic configurations. This was done for 20 nm-thick iron nanodots with different diameters (30, 40, 65, and 80 nm) as a function of applied magnetic field. By analyzing the energy landscape for different magnetic configurations, we calculated the energy barrier for switching from the vortex to the single-domain state (vortex annihilation) and the converse (vortex nucleation). The applied fields required to overcome these two barriers are compared to those obtained from the simulations of the magnetic reversal. The role of the thermal fluctuations in the temperature dependence of these characteristic fields is analyzed by comparison of the energy barriers with the thermal energy, k_BT.

ACKNOWLEDGMENTS

This work is supported by the TAMU-CONACYT collaborative research program. The authors would also like to acknowledge M. Donahue at NIST for his invaluable advice in adapting OOMMF for our uses.

NOMENCLATURE

M	Magnetization
M_s	Saturation Magnetization
H	Applied Magnetic Field
H_a	Annihilation Field
H_n	Nucleation Field
μ_o	Permeability of Free Space
k_B	Boltzmann's Constant
γ	Gyromagnetic Ratio
α	Damping Coefficient
T	Temperature
t	Time
A_E	Exchange Stiffness
K_1	Crystalline Anisotropy Constant
By	Magnetic Field in y-direction
Hy	Applied Magnetic Field in y-direction

TABLE OF CONTENTS

Page

LIST OF FIGURES

FIGURE Page

LIST OF TABLES

CHAPTER I

INTRODUCTION

A bar magnet, magnetized in a single direction, has its magnetic field lines stretching to infinity. There is a magnetic energy associated with this field. In a cylindrical nanodot of a certain size, the magnetization will form closed loops within the boundaries of the dot in order to minimize the magnetic energy. The loops are typically formed in a plane which is parallel to the top surface of the dot. When this occurs, we say that the magnetization of the dot is in the "vortex state." This is, of course, different from the "single-domain state" where the magnetization is mostly collinear.

The magnetic vortex state is proving to possess characteristics which may enable many novel technologies.[1] For example, when a dot is in the vortex state, it has very little magnetic interaction with surrounding dots. This may allow dense packing of dots in order to create high-density magnetic recording media (HDMRM). Also, when the vortex core is displaced, it returns to equilibrium following a damped oscillatory path. It is possible to apply a magnetic field in such a way to drive this oscillation and create high-frequency nano-oscillators.

In order to exploit these technologies, we must understand how the magnetization reacts

---

This thesis follows the style of Physical Review B.

to an applied magnetic field while it is in the vortex state. In addition, we must understand what is required to switch the magnetization between the vortex and single-domain states in terms of an applied magnetic field and the temperature. Our goal is to numerically determine the dependence of the energy barriers upon the applied magnetic field for different dot sizes and to compare the energy barriers to the thermal energy.

In previous experimental work performed by Dumas, et.al.,[2] two characteristic fields relating to vortex nucleation and annihilation were measured as functions of temperature. The two fields, which will be discussed later, were shown to depend upon the temperature of the nanodot. It was suggested that this temperature dependence could be explained by thermally-activated switching between the vortex and non-vortex states. To investigate this, we perform "rigid-vortex" simulations to calculate the energy barriers between the vortex and non-vortex states and then compare these energy barriers to the thermal energy of the system (temperature, T, multiplied by Boltzmann's constant, k_B.

Applications of the vortex state

As mentioned previously, HDMRM technologies may become feasible through use of the vortex-state magnetization. In common magnetic recording media, a single binary bit is stored as the net magnetization of a section of magnetic material. The sections in which bits can be stored are much larger than the grain size of the material but limited in size by the magnetic interactions with other sections. Therefore, in order to further

increase the density of magnetic recording media, we must find a way to overcome this lower limit and decrease the physical volume in which each bit is stored.

One possibility to overcome the lower limit in bit size is to store bits in the vortex state magnetization of nanodots. In this situation, bits may be stored in the chirality of the vortex: clockwise for a binary "1" or counter-clockwise for a binary "0". Alternatively, a bit could be stored in the out of plane magnetization which occurs at the vortex core: up for a binary "1" or down for a binary "0". By positioning the vortex core close to the center of the dot, the net magnetization of a nanodot can be made small therefore reducing the magnetic interactions between nanodots. This allows more spatially dense packing of nanodots and therefore HDMRM.

Now we turn to the dynamic properties of the vortex state. When a magnetic field is gradually applied to a nanodot initially in the vortex state, the magnetization will begin to align along the field. In order for this alignment to happen, the vortex core moves in a direction perpendicular to the applied field, therefore leading to a net magnetization in the direction of the applied field. Then, when the applied field is removed, the vortex core will begin to move back to the center of the dot. However, the vortex core does not follow a straight line toward the center of the dot, instead it precesses. The trajectory through which the vortex core precesses is similar to a decaying orbit about equilibrium. By periodically applying a magnetic field in such a way that it cancels out the damping

forces, the vortex core can be made to move in a circular, oscillatory path about the center of the dot. This is an example of a high frequency magnetic oscillator.

Method of simulation

Measurement of the magnetization of a bulk material produces a continuous magnetization across the material on the macroscopic scale. It could be assumed that this magnetization is still continuous on smaller scales, however this is not the case. The magnetization of a material is defined as the sum of all the magnetic moments in the material divided by the volume of the material. A calculation of the magnetization of a material would involve all the magnetic moments of the individual atoms and the interactions between them. However, this calculation is unreasonable due to the extreme number of atoms in a bulk material.

A useful simplification to this calculation is to assume that the interactions between electron spins are sufficiently strong to prevent any significant change in the orientation of the adjacent spins and therefore allow approximation by continuous functions.[3] From this assumption, we can reduce the problem to a much simpler problem of magnetic cells defined as regions of a material where the magnetization does not vary with position. Each cell typically contains a large number of electron spins. Therefore, this "micromagnetic" theory provides a much simpler method of calculation using the Landau-Lifshitz equation[4] and the Brown energy equations.[3]

The equations of micromagnetic theory are in the form of partial differential equations which cannot be solved analytically.[3] Fortunately, the National Institute of Standards and Technology (NIST) has developed the Object Oriented Micromagnetic Framework (OOMMF) to solve the micromagnetic equations numerically.[5] In standard operation, OOMMF minimizes the total magnetic energy of the system over time, eventually settling down to a lowest-energy state and calculating the magnetization. In addition to the magnetization, OOMMF also calculates several other parameters including the various magnetic energies as defined by W.F. Brown.[3] We adapted OOMMF to numerically calculate the total magnetic energy of various states of magnetization that we define, which may or may not be the ground state.

We apply a "rigid vortex approximation" (Ref. 6) with OOMMF to obtain an energy landscape for switching between the single-domain and vortex states. From the energy landscape, we then calculate the energy barriers between these two states. To evaluate the accuracy of the rigid-vortex method, we will also be using OOMMF to perform standard magnetization curve simulations, with which we will compare our rigid-vortex results. We will refer to the magnetization curve simulations as hysteresis simulations.

Project overview

The dependence of the energy barriers upon applied field was determined through micromagnetic simulations using the rigid-vortex approximation. The dependencies

demonstrate two characteristic fields: the field at which the nanodot switches from the vortex state into the single-domain state (vortex annihilation field, H_a) and the field at which the nanodot switches from the single-domain state into the vortex state (vortex nucleation field, H_n).

Additionally, the energy barriers were compared to the thermal energy defined as the temperature (T) multiplied by Boltzmann's constant (k_B). This comparison demonstrates the likelihood of the thermal fluctuations to overcome the energy barriers and cause switching between states.

The applications described in the earlier section require knowledge of the two characteristic fields, H_n and H_a, and the thermal stability of the magnetization states of nanodots. Therefore, the dependencies found will help to further these and many other technologies as well as to understand the fundamental physics behind the magnetic state switching.

CHAPTER II

METHODS

Micromagnetic theory

As mentioned previously, in order to rigorously determine the magnetization of a material, we must have knowledge of each magnetic moment in the material. Consequently, the problem becomes extraordinarily difficult in a bulk material with countless magnetic moments. If we can reduce the number of moments in the calculation, we will greatly simplify the problem.

If we make the assumption that the individual magnetic moments only slightly deviate in orientation from their neighbors, then the magnetization will vary smoothly throughout the material. Therefore, we can group large numbers of magnetic moments into "cells" defined by regions where the magnetization does not vary with position. This allows us to approximate large numbers of moments nearly as a single cell with the combined magnetic moment. Since the physical scale of the cells is typically several orders of magnitude larger than that of a single spin, this approximation greatly simplifies the calculation. W. F. Brown derived the equations for the magnetic energies[3] that we use in this work.

Also, since we are assuming the magnetization varies smoothly with position, we are allowed an approximation by continuous functions. Therefore, we are allowed to use the Landau-Lifshitz equation.[4]

$$\frac{d\vec{M}}{dt} = -\gamma \vec{M} \times \vec{H}_{eff} - \frac{\gamma\alpha}{M_s} \vec{M} \times (\vec{M} \times \vec{H}_{eff}) \tag{2.1}$$

The Brown energy equations, shown below, depend upon the magnetization, the applied field, and several material parameters. The exchange energy is given by,

$$E_{ex} = \frac{A}{M_s^2} \int (\nabla M)^2 dV \tag{2.2}$$

the demagnetization energy is given by,

$$E_d = \frac{\mu_o}{2} \iint M(r) N(r - r') M(r') dV' dV = \frac{\mu_o}{2} \int H_d \cdot M(r) dV \tag{2.3}$$

the anisotropy energy is given by,

$$E_{an} = -\frac{1}{2} \int M \cdot \Lambda \cdot M dV \tag{2.4}$$

the Zeeman energy is given by,

$$E_Z = -\mu_o \int H_{Zeeman} M dV \tag{2.5}$$

and the total energy is given by,

$$E_{tot} = E_{ex} + E_d + E_{an} + E_Z \tag{2.6}$$

Since, the applied field and the material parameters are known, the only unknown is the magnetization at a given time. So, if we solve the Landau-Lifshitz equation for the magnetization at each time step, then we cause use the result in the Brown energy equations to calculate the magnetic energies at discrete points in time.

Object-oriented micromagnetic framework

The Object Oriented Micromagnetic Framework (OOMMF) was developed by the National Institute of Standards and Technology (NIST) in order to solve the Landau-Lifshitz equation numerically. We used the January 15, 2004 release of the OOMMF 2D solver version 1.1 beta 2 running with Tcl/Tk version 8.5.7 on Mac OS X 10.6. OOMMF begins with a given initial magnetization and a known applied magnetic field. The gyromagnetic ratio, the fine-structure constant, and the saturation magnetization are all also given to OOMMF as initial conditions. These variables are then used to calculate the first time derivative of the magnetization from the Landau-Lifshitz equation. Next, the time derivative is integrated over one time step and plugged back into the Landau-Lifshitz equation. This process continues until the magnetic torque term, $\vec{M} \times \vec{H}_{eff}$, reaches a predefined minimum known as a control point or after a specified number of iterations. At this point, it is assumed that the system reaches the equilibrium state, which is recorded. Then the magnetic field is changed and the new magnetic state is calculated.

Rigid-vortex approximation

The magnetization states that we will simulate are the vortex state and the single-domain state. The vortex state occurs when the in-plane magnetization curls around a fixed point, and the single domain-state occurs when the magnetization is mostly collinear. Our goal is to understand, how the switching between the two states occurs. Our objective is to calculate the fields required to switch into the vortex state and into the

single-domain state. These are known as the vortex nucleation (H_n) and annihilation fields (H_a), respectively.

To perform our calculations, we have employed a "rigid vortex approximation." In this approximation, we assume that the vortex shape does not change as a function of the vortex position. This allows us to model different magnetization states by placing the vortex core at various positions with respect to the dot.[6] As we move the vortex core from the center of the dot to far away from the dot, we obtain an evolution of magnetization states. The single-domain state corresponds to placing the vortex core far away from the dot, while the vortex state corresponds to placing the vortex core within the dot. The vortex positions in between represent the evolution the system is likely to follow in order to switch from the vortex to the single-domain state or vice versa. By calculating the total magnetic energy for each position of the vortex core, we will obtain a landscape of the magnetic energies that the system is likely to follow in order to switch between states. For a range of the nanodot parameters, there are two energy minima, separated by a peak, corresponding to the vortex and single-domain states.[7] This peak creates an energy barrier for switching between the vortex and single-domain states. When a magnetic field is applied, the energy landscape changes. The field at which the energy of the single-domain state becomes greater than the peak and causes the energy barrier to disappear is the vortex nucleation field (H_n). On the other hand, the field at which the energy of the vortex state becomes greater than the peak and causes the energy barrier to disappear is the vortex annihilation field (H_a).

OOMMF adaptation

In order to use the rigid vortex approximation, we had to adapt OOMMF to our procedure. Normally, OOMMF allows the magnetization to relax before it records any data. This may take many iterations and will never record any data about the initial state such as the values of the magnetic energy. However, in the rigid vortex approximation, we do not want the system to relax. This is because the system would fall into a stable state and we would not be able to calculate an energy landscape. Instead, we must calculate the magnetic energies regardless of how unstable the state. Therefore, we wrote a program in C to control OOMMF in a way so that we could calculate the magnetic energies at whatever state we define, no matter how unstable. We also added a feature in this C program which would automatically sort the data into files which could be read easily by Microsoft Excel to be analyzed.

CHAPTER III

RESULTS

In this work, we perform two types of simulations. The first type of simulation is the straight-forward hysteresis simulation using OOMMF in standard operation. The second, is performed using the rigid-vortex approximation along with the prewritten C-code to automate OOMMF as described in the previous chapter. We will refer to the first type of simulations as "hysteresis simulations," and the second type as "rigid-vortex simulations."

In both types of simulations we kept the following parameters the same. The nanodots are defined to consist of iron with a saturation magnetization (M_s) of 1700×10^3 A/m^3, an exchange stiffness (A_E) of 22×10^{-12} J/m, a damping coefficient (α) of 0.5, and a gyromagnetic ratio (γ) of 2.21×10^5 m/(As). The anisotropy is uniaxial and constant, with the crystalline anisotropy axes on the x and y axes and with a crystalline anisotropy constant (K_1) of 48×10^3 J/m^3. The algorithm for calculating the self-magnetostatic (demagnetization) field is set to ConstMag as described in the OOMMF documentation.[5] All nanodots in the simulations have a cylindrical geometry with a 20 nm height, and the diameters of the nanodots are varied between 30, 40, 65, and 80 nm.

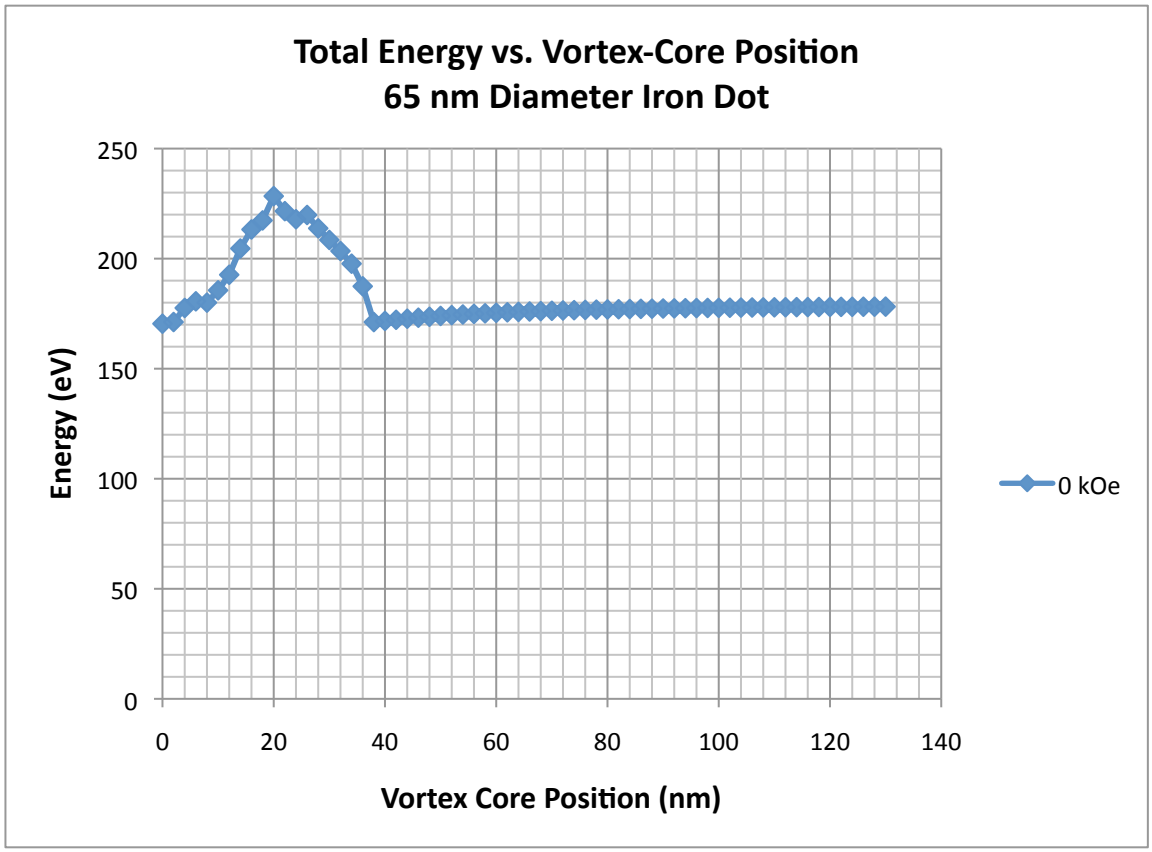

FIG. 1. Energy landscape for a nanodot with a 65 nm diameter at zero applied field. This plot was calculated using the rigid-vortex approximation along with OOMMF.

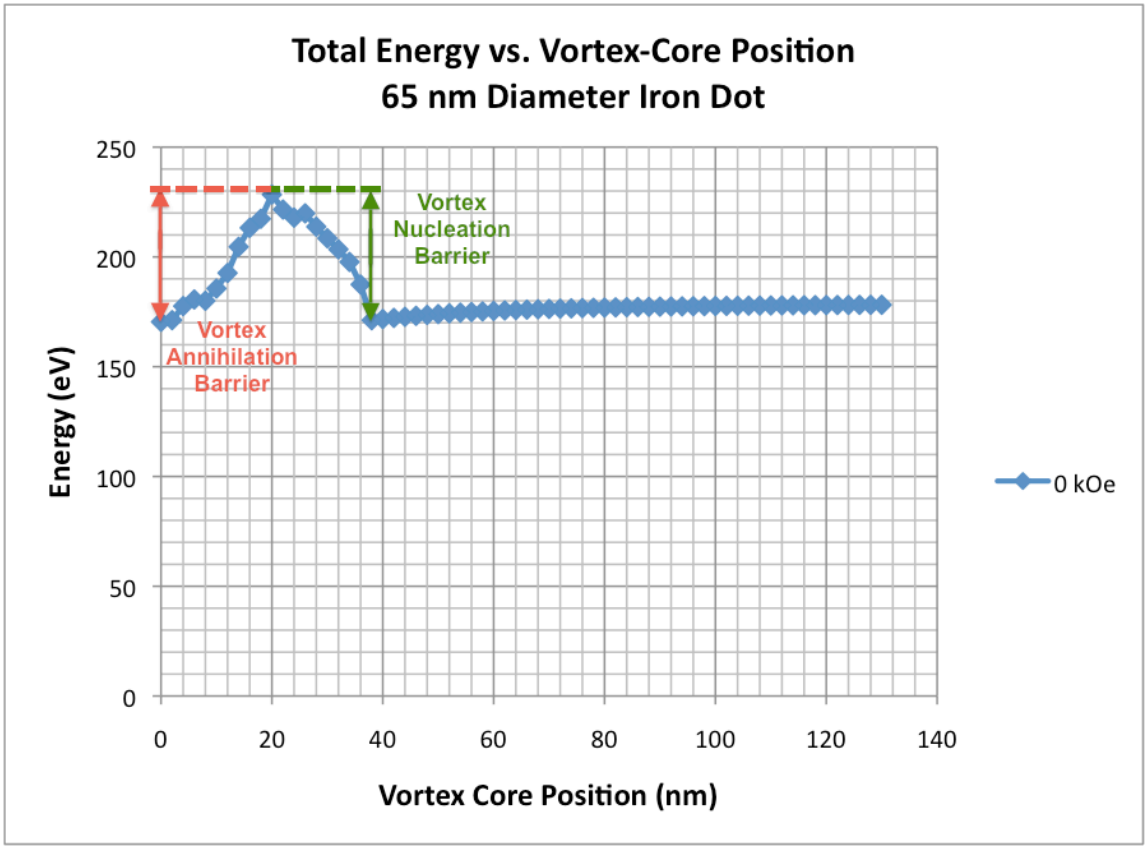

FIG. 2. Sketch of the vortex nucleation and annihilation energy barriers. The annihilation barrier is shown in red and the nucleation barrier is shown in green.

Rigid-vortex simulations

In all rigid-vortex simulations, the vortex-core radius is fixed at 8 nm. All magnetization outside the vortex-core is in plane, and all the magnetization within the vortex-core points out of plane.

When the rigid vortex approximation is applied to calculate the magnetic energies of a nanodot with respect to vortex-core position, we find an energy landscape. Figure 1

shows the energy landscape of a nanodot with a 65 nm diameter with no applied magnetic field. From this plot, the vortex nucleation and annihilation barriers can be calculated. These two energy barriers are sketched in Figure 2.

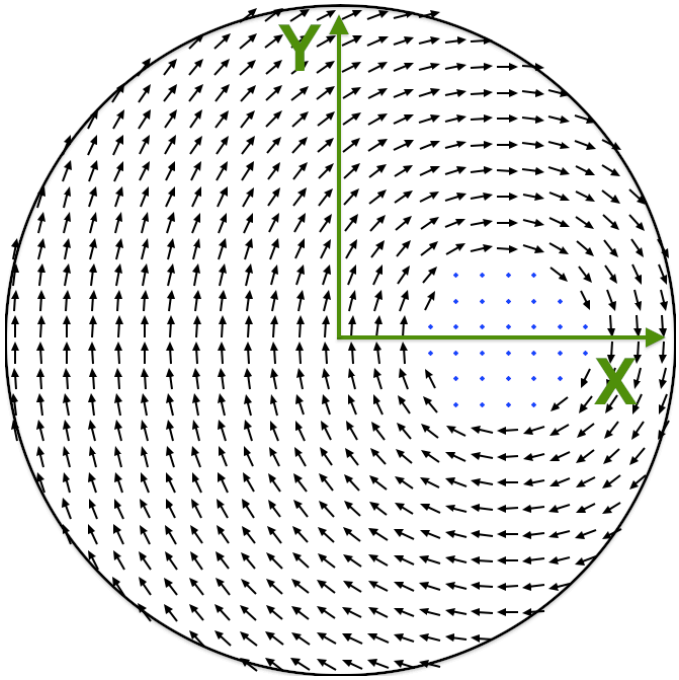

FIG. 3. Sketch of a top-down view of a nanodot defining the x-axis as the axis along which the vortex-core moves. The y-axis is defined as the axis in the same plane, but orthogonal to, the x-axis. All applied fields are parallel to the y-axis. The vector field represents the magnetization of the nanodot; the black arrows are in plane and blue arrows are out of plane.

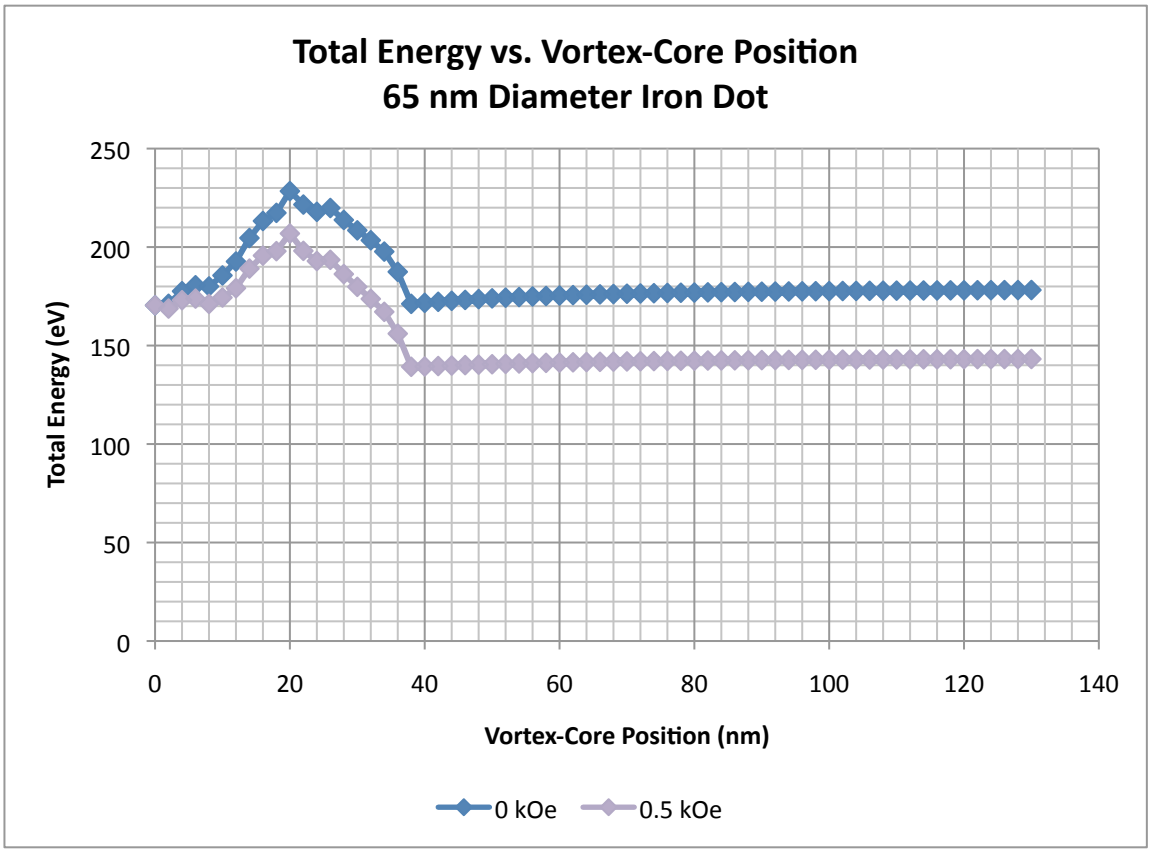

FIG. 4. Energy landscapes for a nanodot with a 65 nm diameter at zero and 0.5 kOe applied field. Calculated using the rigid-vortex approximation with OOMMF.

By defining the axis along which the vortex-core is moved to be the in-plane x-axis, we can apply a magnetic field along what would be the in-plane y-axis. This is sketched in Figure 3. When a positive field is applied with the geometry in Figure 3 and the energy landscape is recalculated, we would expect the annihilation barrier and the total energy of the non-vortex state to decrease. This is because the magnetic moments tend to align along the applied field, favoring a collinear, single-domain state. This can be seen in Figure 4, where an energy landscape at 0.5 kOe is plotted along with the energy landscape at zero applied field. After repeating this process for a range of applied fields, we obtain the results shown in Figure 5. Now, the energy landscapes have been calculated at many different applied fields, and we can extract and plot the energy barriers as a function of applied field. This is shown for all four dot diameters in Figures 6 through 9.

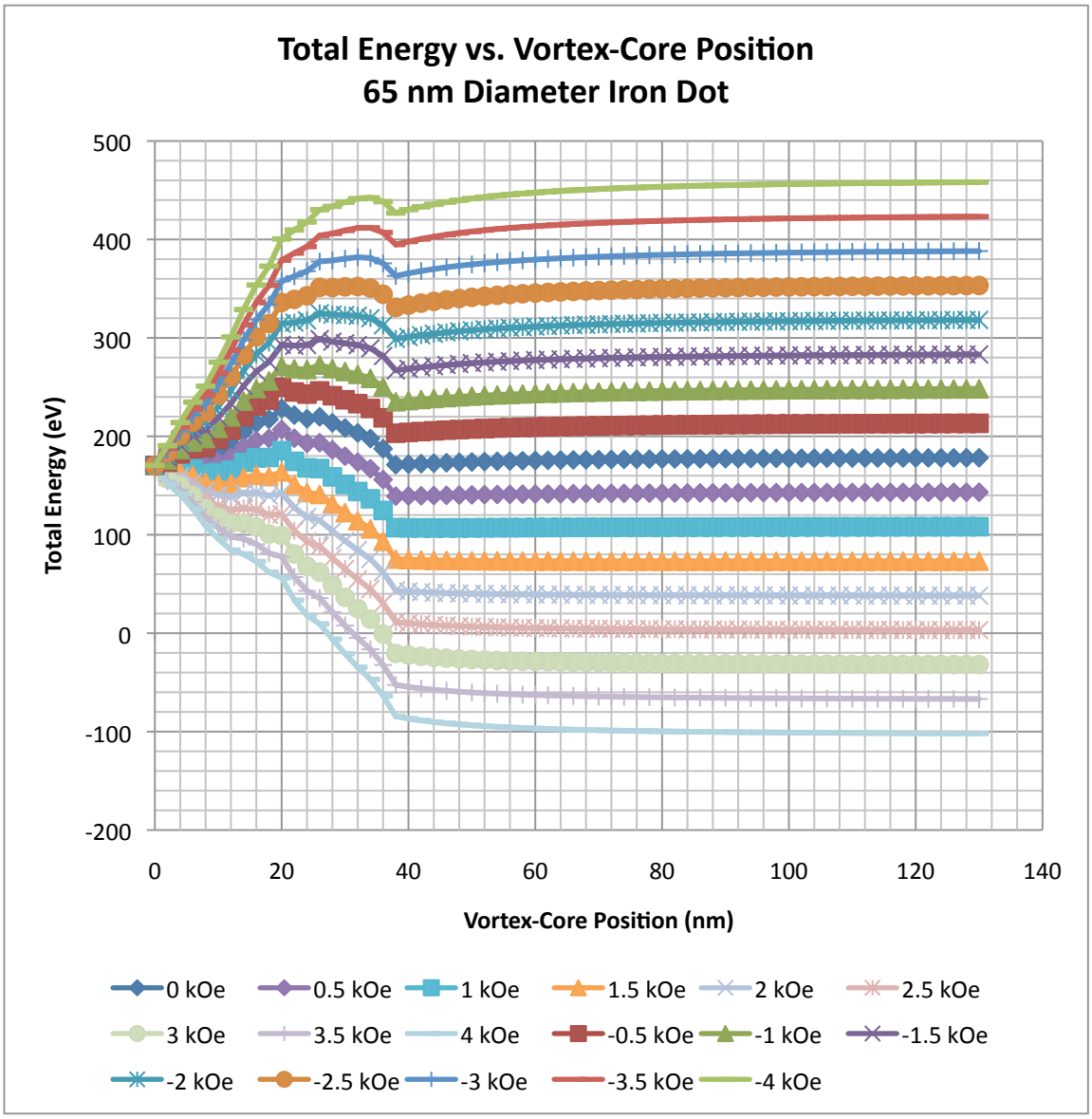

FIG. 5. Energy landscapes for a nanodot with a 65 nm diameter at many different applied fields.

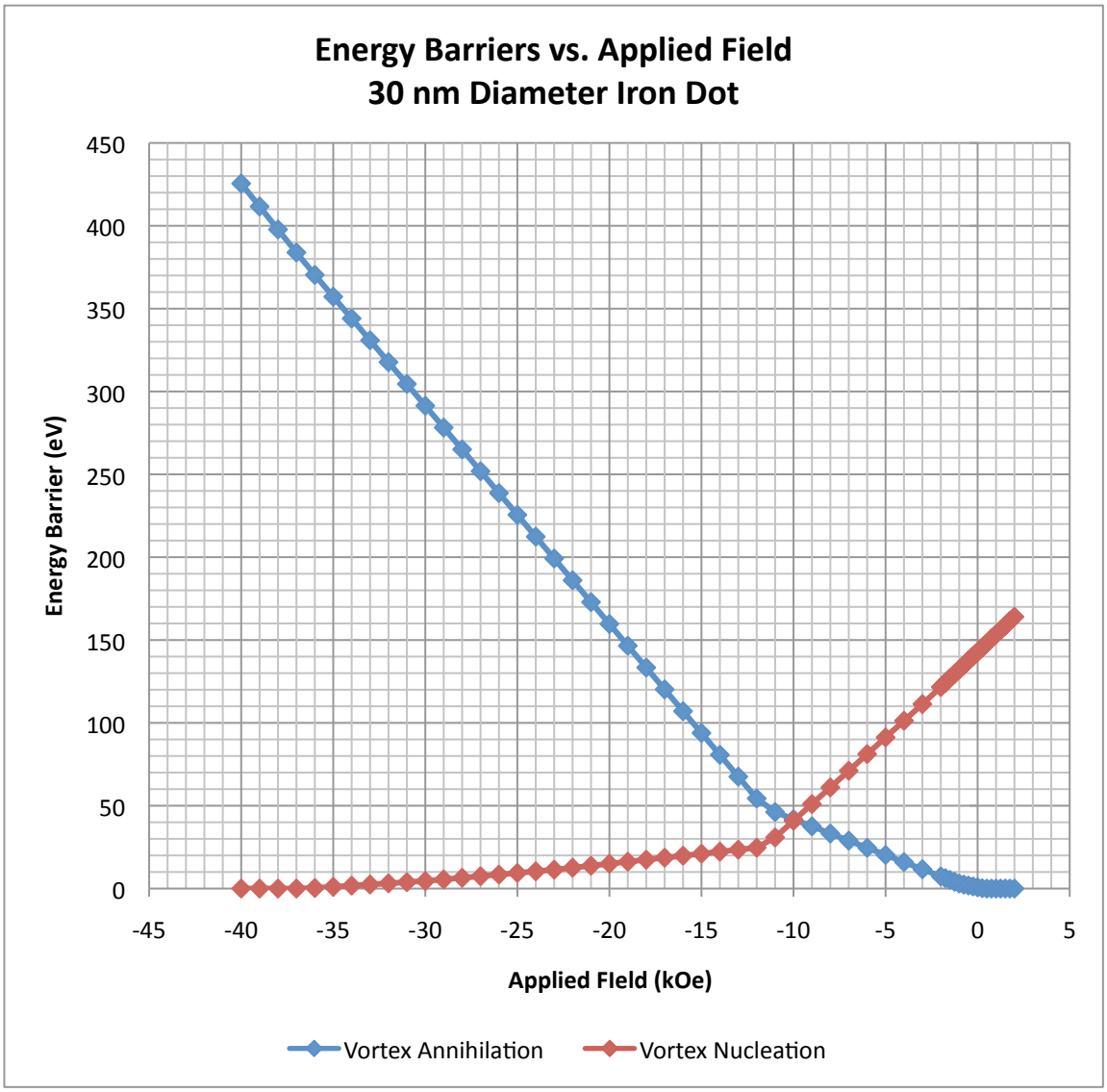

FIG. 6. Energy barriers plotted versus applied field for a nanodot with a 30 nm diameter. This was calculated using the rigid-vortex approximation with OOMMF.

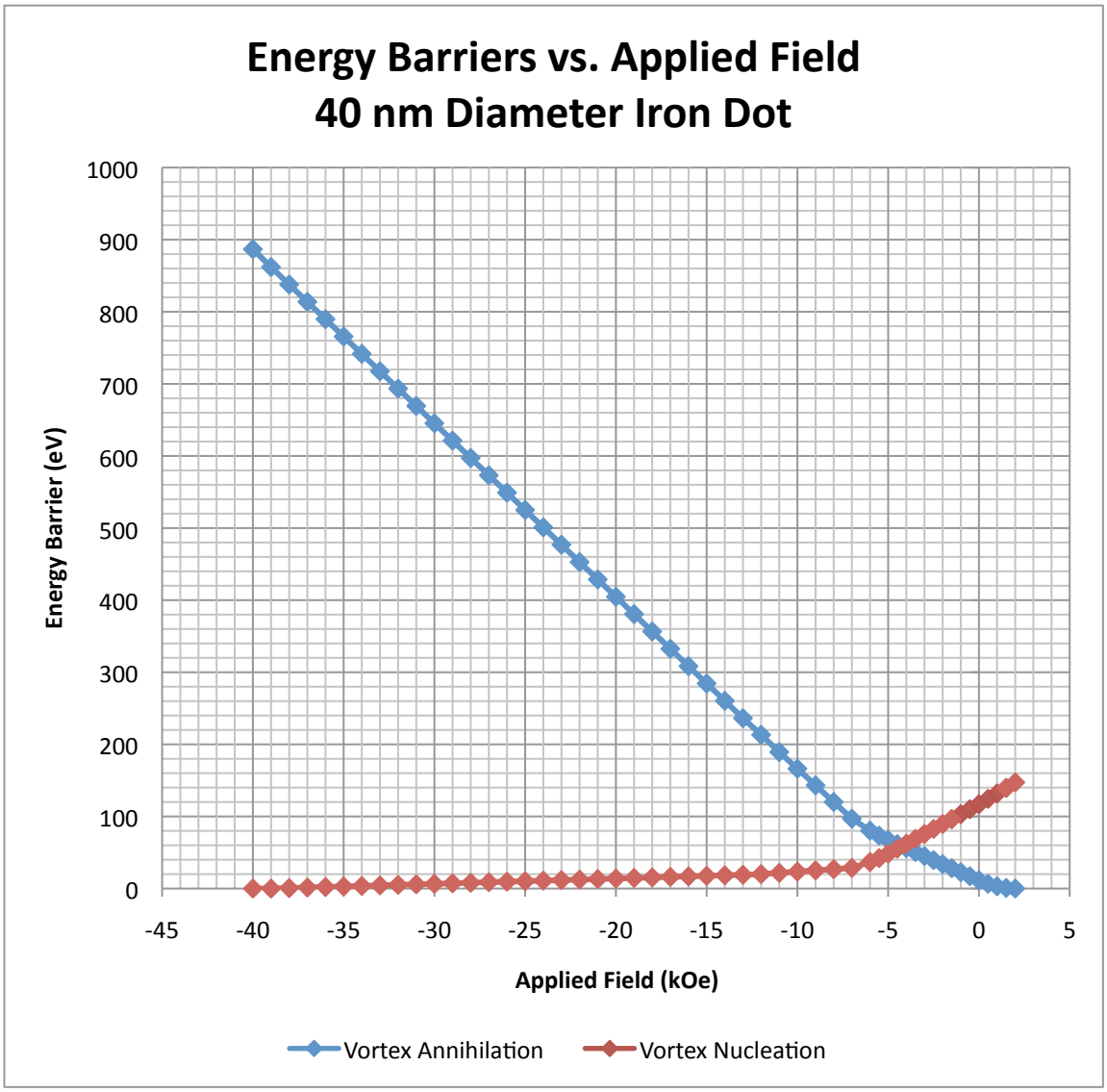

FIG. 7. Energy barriers plotted versus applied field for a nanodot with a 40 nm diameter. This was calculated using the rigid-vortex approximation with OOMMF.

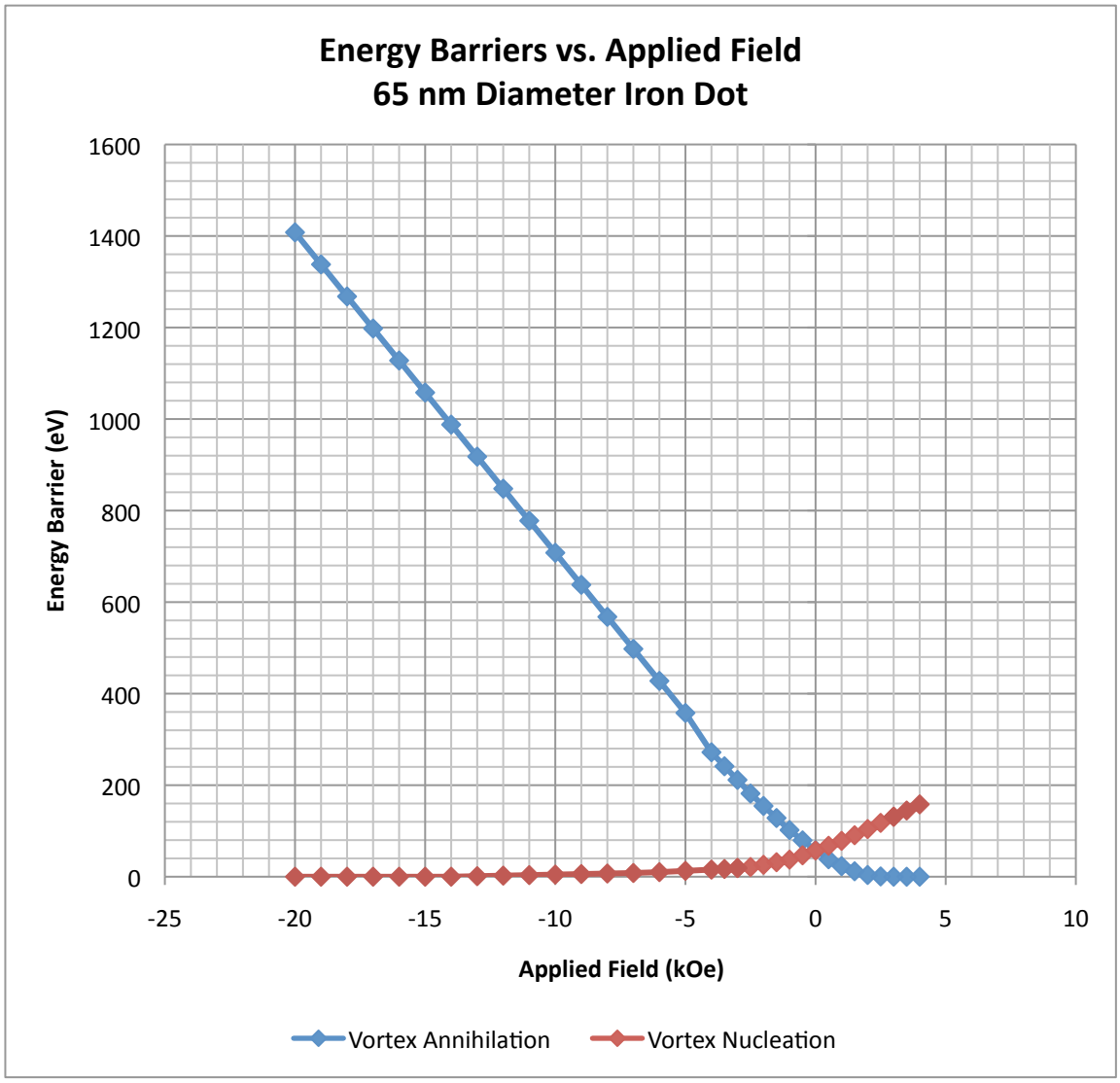

FIG. 8. Energy barriers plotted versus applied field for a nanodot with a 65 nm diameter. This was calculated using the rigid-vortex approximation with OOMMF.

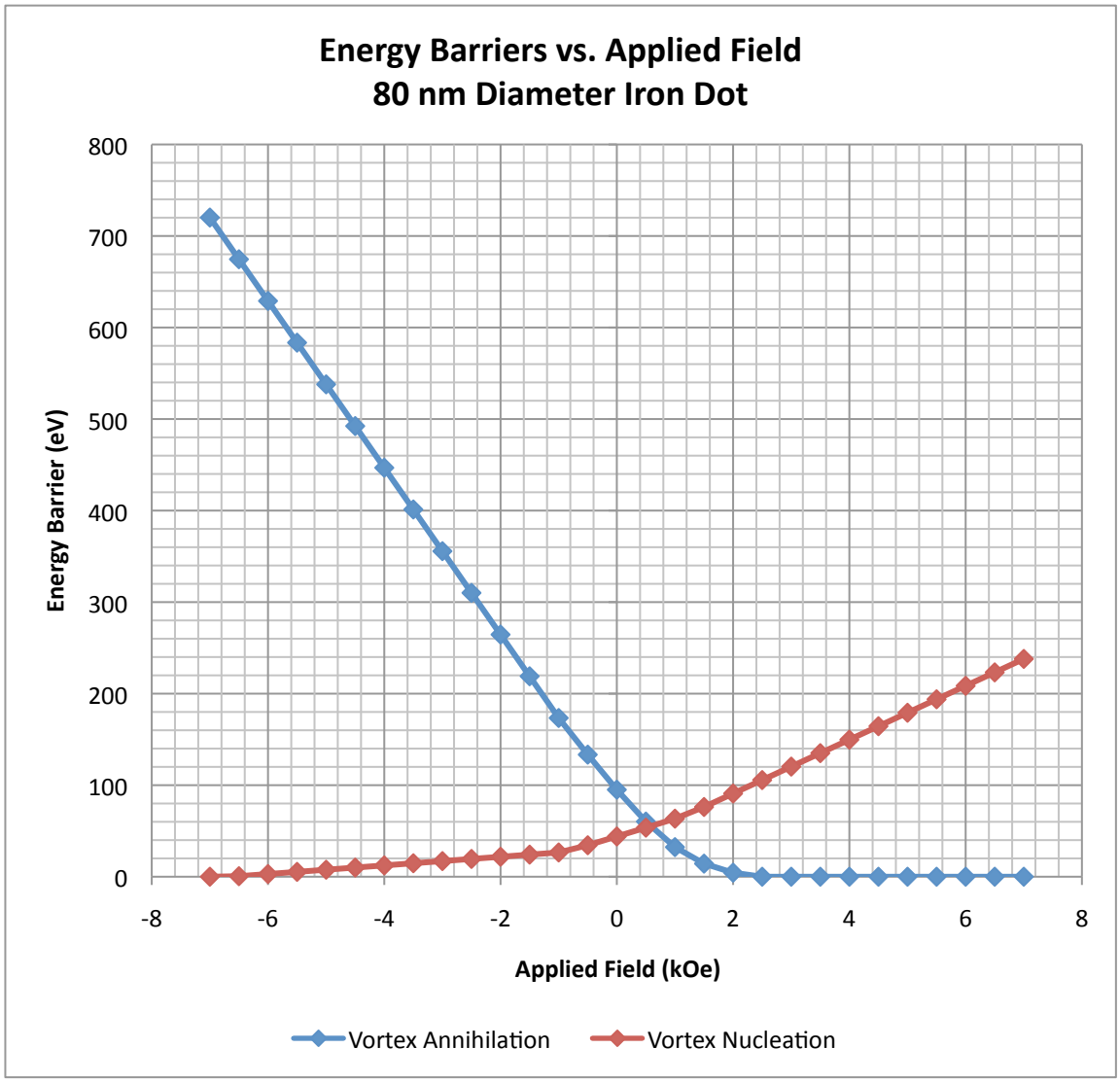

FIG. 9. Energy barriers plotted versus applied field for a nanodot with an 80 nm diameter. This was calculated using the rigid-vortex approximation with OOMMF.

As mentioned in the previous chapter, the vortex nucleation or annihilation field, at zero temperature, is defined as the applied field at which the respective energy barrier goes to zero. Therefore, the two characteristic fields are extracted from Figures 6 through 9 and plotted as a function of dot diameter in Figures 10 and 11.

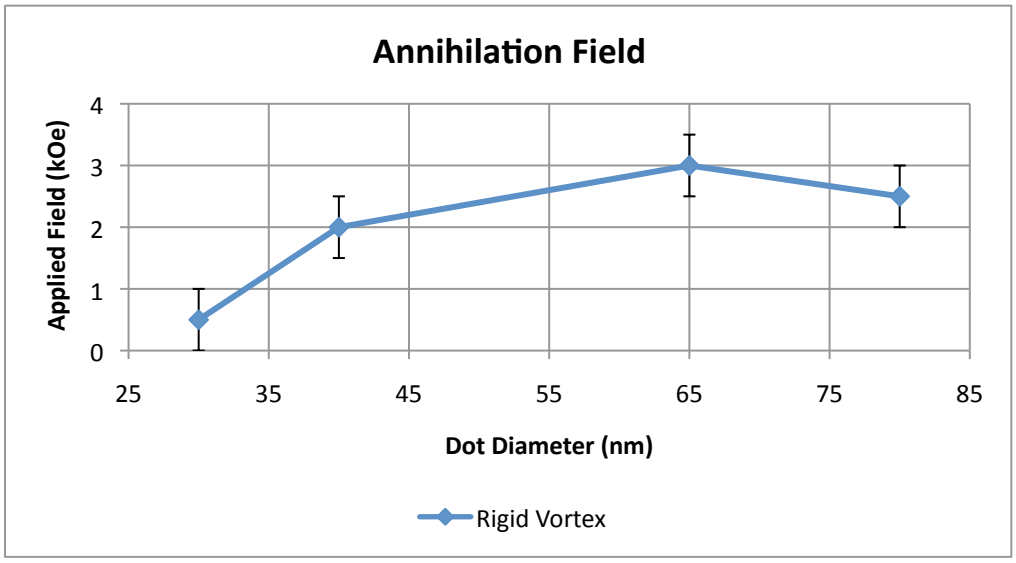

FIG. 10. Vortex annihilation fields plotted versus dot diameter. This was calculated using the rigid-vortex approximation with OOMMF.

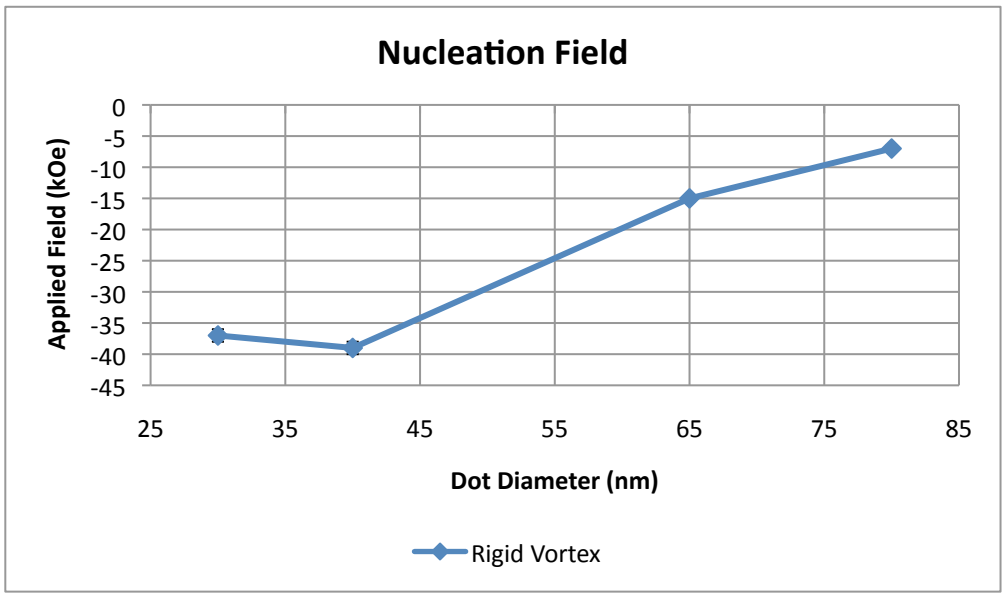

FIG. 11. Vortex nucleation field plotted versus dot diameter. This was calculated using the rigid-vortex approximation with OOMMF.

Hysteresis simulations

For the hysteresis simulations, the initial magnetization state is defined to be the vortex state and a magnetic field is applied to simulate a full hysteresis loop. The magnetic field is initially set to zero until OOMMF reaches a control point as described in the previous chapter. Then, the applied field is changed according to the values in Table 1. Note that there is a small applied field component along the x-axis in order to break the symmetry of the system so that the vortex-core could be displaced from the center of the dot. The results of the hysteresis simulations are shown in Figures 12 through 15. Note that the horizontal axes in Figures 12 through 15 are labeled "By (mT)." This is different from the rigid-vortex data, in which we used "Applied Field (kOe)." If we let "Hy (kOe)" represent the applied field in the rigid-vortex data, then $By = \mu_o Hy$, where μ_o is the vacuum permeability, and 1 kOe corresponds to 100 mT.

TABLE 1. Applied field ranges used in hysteresis simulations. The field begins on the first line in the table at the initial value of (X(1),Y(1),Z(1)) then changes the next values, (X(2),Y(2),Z(2)), taking the specified number of steps along the way. Then, when a control point is reached, the field performs a similar routine with the values on the next line in the table. This simulation ends after the last line in the chart.

X(1) [mT]	Y(1) [mT]	Z(1) [mT]	X(2) [mT]	Y(2) [mT]	Z(2) [mT]	Steps
0	0	0	0	0	0	1
0	0	0	0.10	300.	0	40
0.10	300.	0	0.10	400.	0	20
0.10	400.	0	0.10	300.	0	20
0.10	300.	0	0	0	0	40
0	0	0	-0.10	-300.	0	40
-0.10	-300.	0	-0.10	-400.	0	20
-0.10	-400.	0	-0.10	-300.	0	20
-0.10	-300.	0	0	0	0	40
0	0	0	0.10	400.	0	60

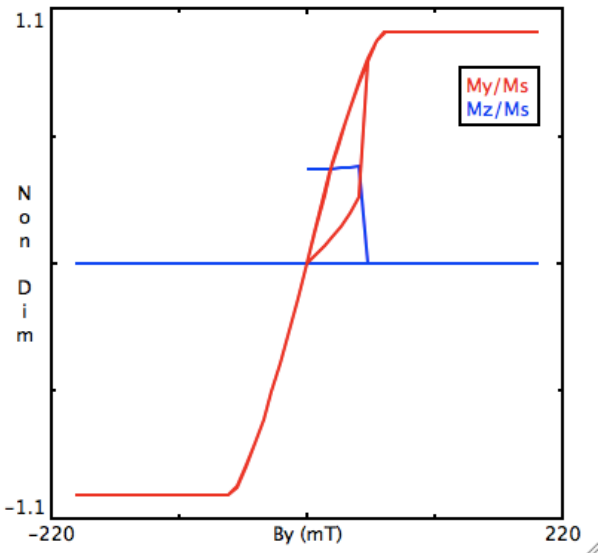

FIG. 12. Hysteresis loop for a nanodot with a 30 nm diameter. This was calculated using OOMMF.

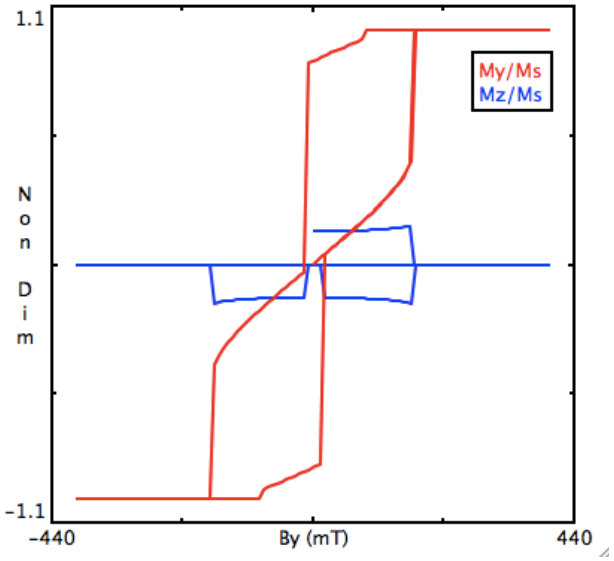

FIG. 13. Hysteresis loop for a nanodot with a 40 nm diameter. This was calculated using OOMMF.

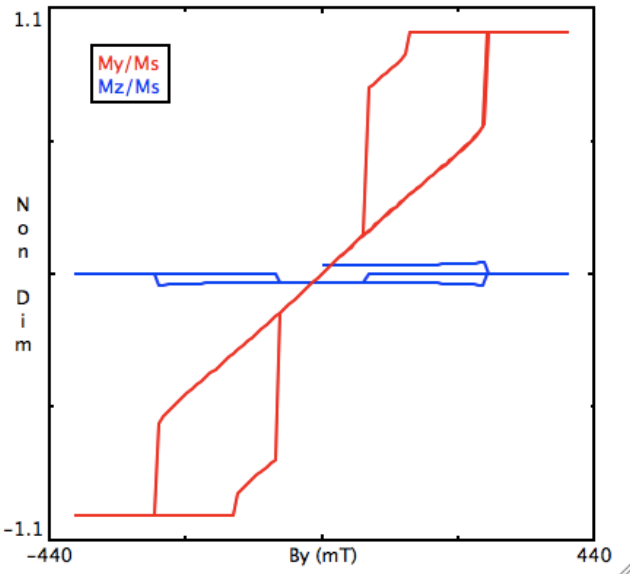

FIG. 14. Hysteresis loop for a nanodot with a 65 nm diameter. This was calculated using OOMMF.

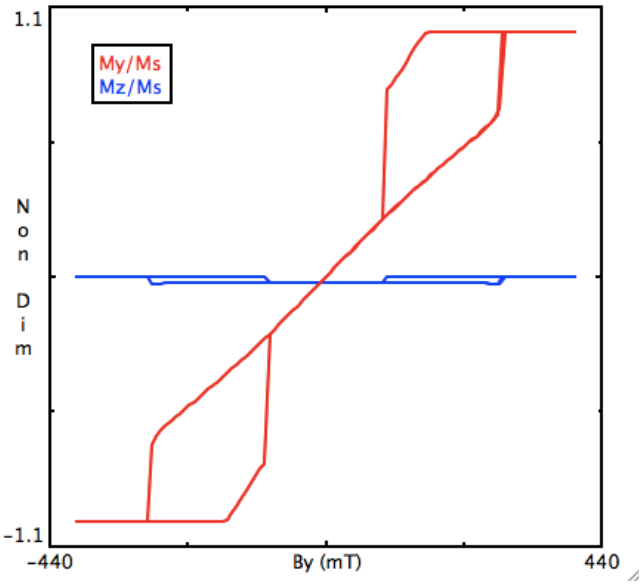

FIG. 15. Hysteresis loop for a nanodot with an 80 nm diameter. This was calculated using OOMMF.

The hysteresis loops appear to be "pinched". This "pinching" is indicative of the vortex state.[8, 9] The vortex annihilation and nucleation fields are then extracted from the hysteresis plots in Figures 12 through 15 as sketched in Figure 16. The two characteristic fields are then plotted as a function of dot diameter in Figures 17 and 18.

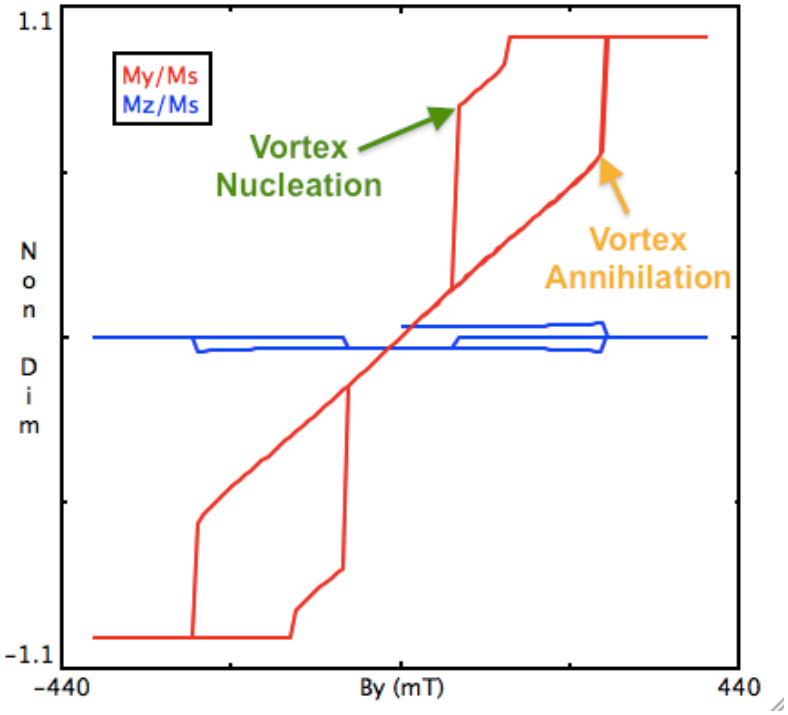

FIG. 16. Sketch of where vortex nucleation and annihilation occurs in the hysteresis loop. The vortex nucleation and annihilation fields are extracted from the hysteresis loop at the points sketched in the plot.

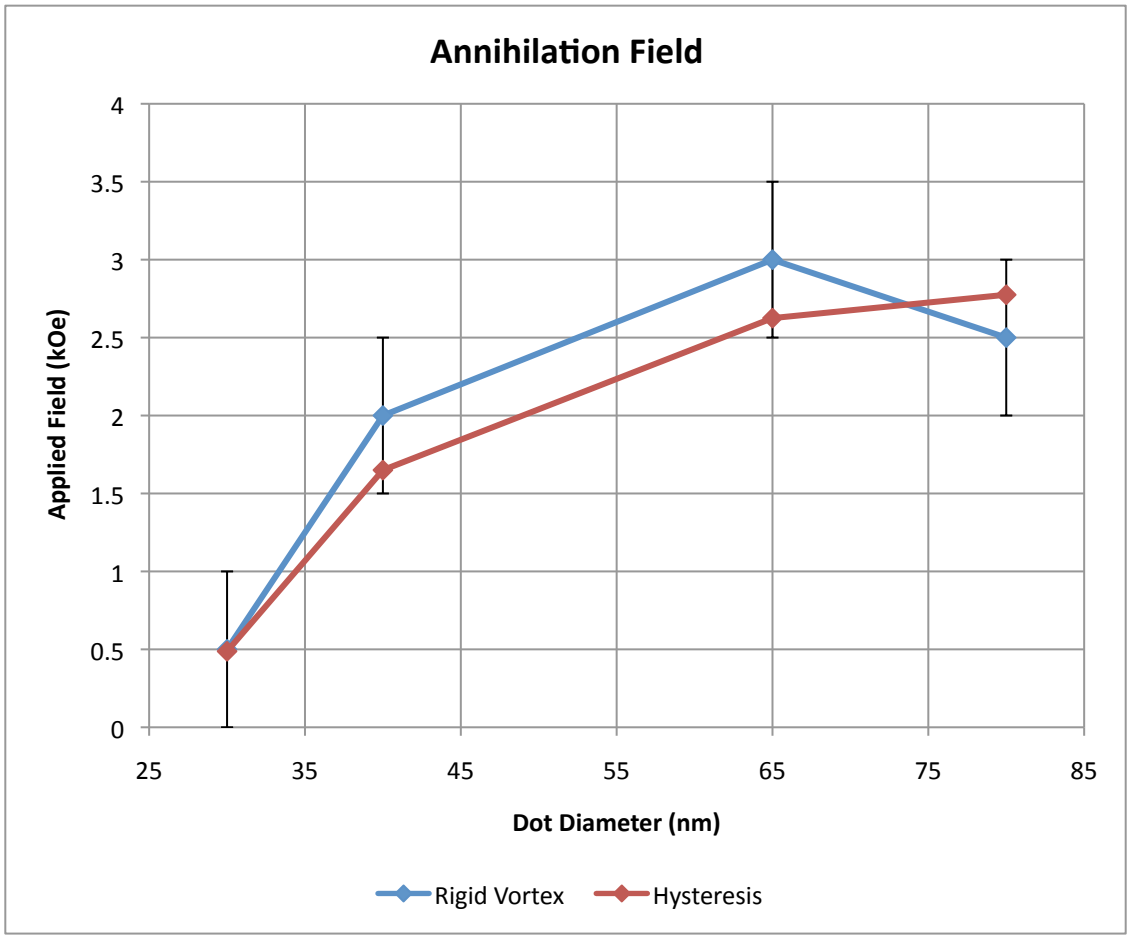

FIG. 17. Vortex annihilation field plotted versus dot diameter. The results from both the hysteresis and rigid-vortex simulations are shown for comparison. The uncertainty bars from the hysteresis simulations are so small that they cannot be seen on the plot. However, the uncertainty bars from the rigid-vortex simulations can be seen.

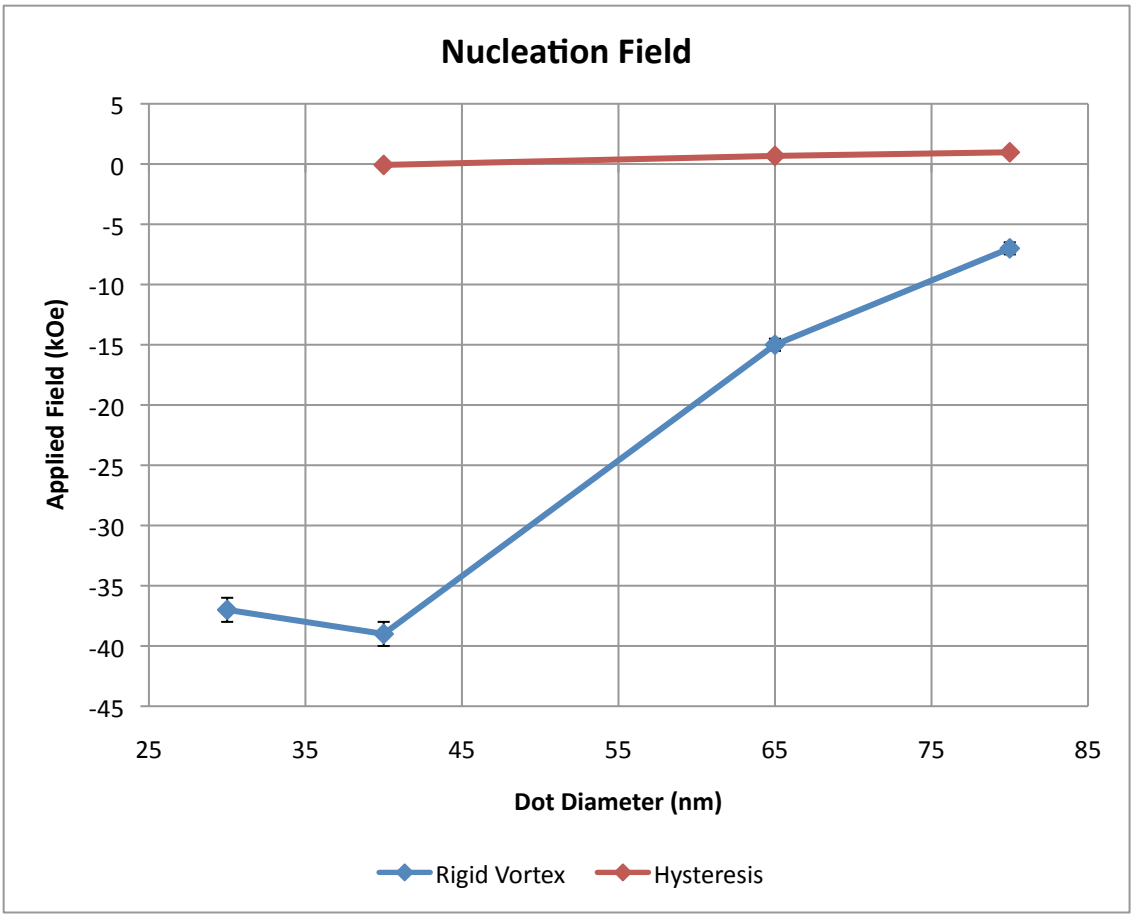

FIG. 18. Vortex nucleation field plotted versus dot diameter. The results from both the hysteresis and rigid-vortex simulations are shown for comparison. The uncertainty bars from the hysteresis simulations are so small that they cannot be seen on the plot. However, the uncertainty bars from the rigid-vortex simulations can be seen.

Notice how, in the hysteresis results, there are no recorded values for the vortex nucleation fields of the nanodot with a 30 nm diameter. This is because, as seen from the simulations of the hysteresis loops for this dot, a vortex will never nucleate. Therefore, there can not be a vortex nucleation field for these nanodots.

CHAPTER IV

CONCLUSIONS & FUTURE OUTLOOK

Comparison with hysteresis

In Figures 17 and 18, the vortex nucleation and annihilation fields from the rigid-vortex simulations are compared to those from the hysteresis simulations. The method of simulating a hysteresis loop is well-established in the field of micromagnetics. Therefore, if the results from the rigid-vortex approach agree with those from the hysteresis approach, then it is reasonable to believe that use of the rigid-vortex approximation is an acceptable approach to studying vortex nucleation and annihilation. Indeed, the sole reason for performing hysteresis simulations is to make this comparison.

It can be seen from Figures 17 that the results for the vortex annihilation fields from the hysteresis simulations are within the uncertainty bounds of the rigid-vortex simulations, indicating that the two results are in agreement. Therefore, we believe the use of the rigid-vortex approximation is an acceptable approach to studying vortex annihilation in nanodots.

We note that, in Figure 18, there is no value for the vortex nucleation field for a nanodot with a 30 nm diameter. This is because, when simulating a hysteresis, OOMMF allows the system to relax. If the vortex state is unstable, then the system will never relax into the vortex state. Therefore, there will be no vortex nucleation field. However, for the

nanodots with 40, 65, and 80 nm diameters, a vortex was able to nucleate, but the results found from the hysteresis simulations do not agree with those found from the rigid-vortex simulations. Therefore, we conclude that the rigid-vortex simulations gave inaccurate results for vortex nucleation. This could be due to the crude nature of the vortex model we used in the rigid-vortex simulations.

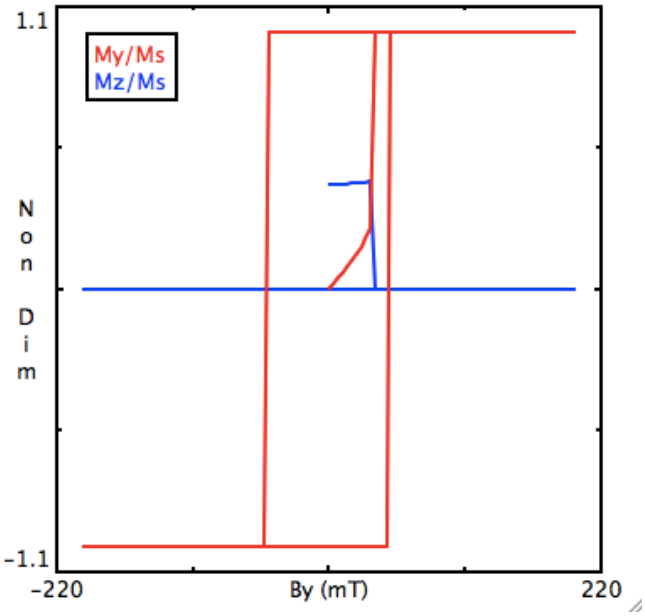

FIG. 19. Hysteresis loop for a nanodot with an 30 nm diameter and uniaxial anisotropy with the easy axis along the applied magnetic field (y-direction). This was calculated using OOMMF.

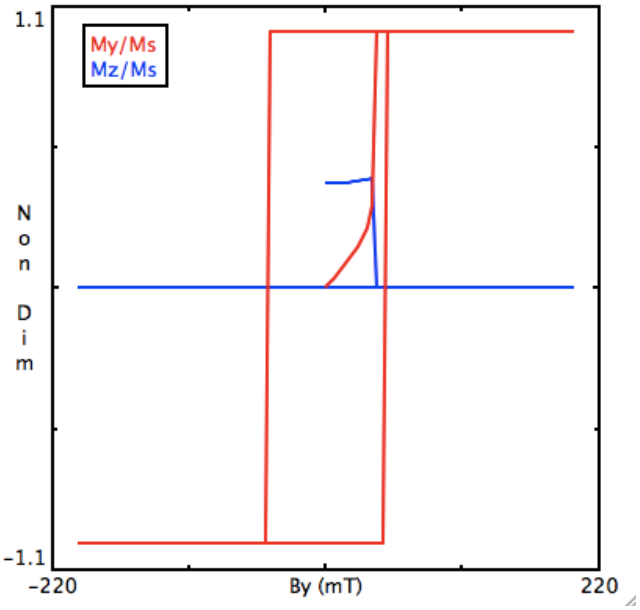

FIG. 20. Hysteresis loop for a nanodot with an 30 nm diameter and cubic anisotropy. This was calculated using OOMMF.

Note that we do not observe hysteresis for the 30 nm diameter nanodot (Figure 12), because we chose the easy axis of the anisotropy to be to be at a 45 degree angle to the applied field. Figure 19 demonstrates that hysteresis is present when the easy axis is along the applied magnetic field (y-direction). Also, even in the case of a cubic anisotropy (Figure 20), which favors the vortex state more than a uniaxial anisotropy,[10] a vortex does not nucleate.

Temperature dependence

In order to study the temperature dependence of the switching between the states calculated in Figures 6 through 9, we use an Arrhenius-type law as seen below in (4.1).

$$\tau = \tau_o * \exp\left(\frac{E_B}{k_B T}\right) \tag{4.1}$$

The constant, τ_o, represents the average time it takes for a nanodot to perform the switching between the vortex and non-vortex states. Typical values for τ_o are in the range of 0.1 ns to 1 ns; for the estimates here, we set τ_o to 1 ns. The time, τ, obtained from (4.1) is the average time before the switching occurs. Within the exponential, we have the ratio between the energy barrier, which depends upon the applied field and the dot diameter, and the thermal energy, which depends upon the temperature. Therefore, for a given dot diameter, we can evaluate (4.1) with respect to two independent parameters: the applied field and the temperature.

Using this approach, we find that the switching time for vortex annihilation in a nanodot with a 65 nm diameter at zero applied field and 300 K would be 6.0×10^{964} seconds. If we increase the applied field to 2.5 kOe, the switching time drops to 64 seconds. Similar results for all four dot diameters are shown in Table 2.

TABLE 2. Switching times for vortex annihilation at particular applied fields and 300 K for all four dot diameters.

Dot diameter (nm)	Applied field (kOe)	Switching time (s)
30	0	3400
30	2	1.0×10^{-9}
40	0	1.8×10^{185}
40	2	1.0×10^{-9}
65	0	6.0×10^{964}
65	2.5	64
80	0	1.8×10^{1588}
80	2.5	1.0×10^{-9}

Table 2 demonstrates that at zero applied field, all the nanodots are stable in the vortex state due to the large switching times, with the exception of the 30 nm diameter dots. However, once a small field is applied, the switching time drastically decreases. We see from Table 2 that the switching times are incredibly large numbers; therefore, we believe that our energy barriers are too large to be reasonable.

To analyze the temperature dependence of the switching times, we need to know the value of the energy barriers. Based upon the evidence discussed above, we conclude that the calculated energy barriers are incorrect, and therefore we are unable to perform a useful analysis.

Our tests indicate that the energy barriers obtained as a result of our model of the vortex state are too large. This means that our model needs to be refined further. In particular, the transition from the vortex core (out-of-plane) magnetization to the in-plane, concentric magnetization outside of the vortex-core is abrupt and causes an increase in

the exchange energy of the system. A refined model with a gradual transition could provide better quantitative results.

Outlook

Although the rigid-vortex approximation gives us reasonable results for vortex annihilation, the discussion from a previous section shows that the rigid-vortex simulations do not give accurate results for vortex nucleation. In order to confirm this, we would like to compare with the results from our collaborators, who are using different computational approaches to solve the same problem.

In the rigid-vortex approximation, we used a model of the vortex state that is not adequate for calculating the energy barriers. In this model, there is a sharp transition in magnetization at the vortex-core circumference. This sharp transition may contribute a large amount of exchange energy to the system, and, since this only occurs in the vortex-state, may be skewing our energy barrier results. Therefore, in the future, we would like to refine our vortex model to have a more gradual transition at the vortex-core radius and then rerun our simulations. This should give us a more realistic estimation of our energy barriers.

REFERENCES

[1] Y. B. Gaididei, V. P. Kravchuk, D. D. Sheka, and F. G. Mertens, J. Low. Temp. Phys **34**, 7 (2008).

[2] R. K. Dumas, C.-P. Li, I. V. Roshchin, I. K. Schuller, and K. Liu, Appl. Phys. Lett. **91** (2007).

[3] W. F. Brown, *Micromagnetics*. (John Wiley & Sons, Inc., New York, 1963).

[4] T. L. Gilbert, Phys. Rev. **100** (1955).

[5] M. J. Donahue and D. G. Porter, NIST, Gaithersburg, MD **NIST 6376** (1999).

[6] K. Y. Guslienko, V. Novosad, and Y. Otani, Appl. Phys. Lett. **78**, 3 (2001).

[7] C.-P. Li, Ph.D. Thesis, University of California San Diego, 2007.

[8] I. V. Roshchin, C.-P. Li, H. Suhl, X. Battle, S. Roy, S. K. Sinha, S. Park, R. Pynn, M. R. Fitzsimmons, J. Mejía-López, D. Altbir, A. H. Romero, and I. K. Schuller, Europhys. Lett. **86** (2009).

[9] J. Mejía-López, D. Altbir, P. Landeros, J. Escrig, A. H. Romero, I. V. Roshchin, C.-P. Li, M. R. Fitzsimmons, X. Battle, and I. K. Schuller, Phys. Rev. B **81**, 8 (2010).

[10] J. Mejia-Lopez, D. Altbir, A. H. Romero, X. Battle, I. V. Roshchin, C.-P. Li, and I. K. Schuller, J. Appl. Phys. **100**, 6 (2006).

CONTACT INFORMATION

Name:	Andrew Thomas King
Professional Address:	c/o Dr. Igor V. Roshchin Department of Physics and Astronomy 4242 TAMU Texas A&M University College Station, TX 77843
Email Address:	mr.andrew.king@gmail.com
Education:	B.S., Physics, Texas A&M University, May 2012 B.S., Mathematics, Texas A&M University, May 2012 Undergraduate Research Scholar